

University of California

Ernest O. Lawrence
Radiation Laboratory

OPTICAL STUDIES OF ELECTROLYTE FILMS ON GAS ELECTRODES

TWO-WEEK LOAN COPY

*This is a Library Circulating Copy
which may be borrowed for two weeks.
For a personal retention copy, call
Tech. Info. Division, Ext. 5545*

DISCLAIMER

This document was prepared as an account of work sponsored by the United States Government. While this document is believed to contain correct information, neither the United States Government nor any agency thereof, nor the Regents of the University of California, nor any of their employees, makes any warranty, express or implied, or assumes any legal responsibility for the accuracy, completeness, or usefulness of any information, apparatus, product, or process disclosed, or represents that its use would not infringe privately owned rights. Reference herein to any specific commercial product, process, or service by its trade name, trademark, manufacturer, or otherwise, does not necessarily constitute or imply its endorsement, recommendation, or favoring by the United States Government or any agency thereof, or the Regents of the University of California. The views and opinions of authors expressed herein do not necessarily state or reflect those of the United States Government or any agency thereof or the Regents of the University of California.

UCRL-16626

J. Electrochemical Society

UNIVERSITY OF CALIFORNIA
Lawrence Radiation Laboratory
Berkeley, California
Contract No. W-7405-eng-48

OPTICAL STUDIES OF ELECTROLYTE FILMS ON GAS ELECTRODES

Rolf H. Muller

December 1965

OPTICAL STUDIES OF ELECTROLYTE FILMS ON GAS ELECTRODES

Rolf H. Muller

Inorganic Materials Research Division, Lawrence Radiation Laboratory
University of California, Berkeley, California, 94720

ABSTRACT

The geometry of stable electrolyte films has been established on nickel and silver surfaces partially immersed in aqueous caustic solutions. Such films, which are very sensitive to factors affecting interfacial energies and may be useful for their determination, appear to be important for the mass transfer in certain gas diffusion electrodes.

The charge transfer at gas-consuming electrodes has long been assumed to occur at the top of the liquid meniscus where the gas, solid and liquid phases, are in contact with each other. Although the concept of such a "line of reaction" leads one to postulate very large local current densities, and early observations by Grove¹ had indicated contributions of a finite electrode area, it was only recently that Wagner and Will called attention to the fact that neither gas diffusion through the bulk liquid near the meniscus nor surface diffusion of adsorbed gaseous species to the liquid phase, where reaction would take place as suggested by Schmid³ and Justi⁴, could account for many experimental results. Will² demonstrated that a relatively large electrode area participated in the electrode reaction. Similar conclusions can be drawn from computations by Iczkowski.⁵ The current distributions determined by Bennion and Tobias⁶ and later by Maget and Roethlein⁷ directly showed the spacial distribution of the electrochemical charge transfer reaction. Theoretical analysis of porous gas diffusion electrodes by Rockett⁸ and Grens⁹ and experiments by Katan et al.¹⁰ have supported the concept of electrolyte films inside pores of some gas electrodes which are of practical interest.

Purpose of this Study

The finite current densities observed away from the apparent electrolyte meniscus suggested the existence of an electrolyte covering on the apparently dry metal surface and it has been the purpose of this work to determine the extent of this electrolyte film on vertically oriented electrodes of simple geometry. In particular, the film thickness, which is an important parameter for the quantitative description of mass transfer on film-bearing gas electrodes, and the factors which affect it were to be studied. The rectangular and cylindrical electrodes employed may be regarded as highly idealized models of the capillaries in a porous body. The study was limited to mechanically polished nickel and silver electrode surfaces for reasons of optical reflection. Only cathodic polarization was employed in order to maintain the properties of the metal surface as much as possible.

Film Interference

Several techniques have been considered for the measurement of electrolyte film thickness as a function of position and time: Mechanical techniques, although independent of electrolyte and electrode materials, result in discontinuous, point-to-point measurements which may not be sensitive enough and also disturb the film. Electrical measurements could be made continuously; however, they depend on the electrolyte conductivity which is not well known and is a function of position. Electrical conductivity measurements also presuppose a uniform film over the test-distance and suffer from disturbance of the object by the probes. Of different optical techniques, light interference was finally chosen because of the possibility of making continuous observations with a

minimum of disturbance to the object, little requirement for uniform film geometry, and good sensitivity for the dimensions involved. A disadvantage of this technique is that it requires a knowledge of the refractive index of the film. The uncertainty of this quantity due to concentration variations, not a priori known, amounts, however, only to a few percent. Light interference for the study of supported liquid films has recently been used by Bascom et al.¹¹ and Deryagin et al.¹²

Film interference, well known from the appearance of soap bubbles or oil spots on water, is due to partial reflection of an incident light wave on front and back sides of the film. The interference causes a tapered film to show, under monochromatic illumination, alternating bright and dark fringes which indicate contour lines spaced at distances corresponding to one wavelength optical path increment. The optical path difference ΔS in the film between interfering reflections depends on refractive index n , film thickness d and angle of refraction ϕ' as shown in Eq. (1). It can also be expressed as a delay in phase, δ_{film} , given in Eq. (2) in radians, where λ is the light wavelength in vacuum.

$$\Delta S = 2 \cdot n \cdot d \cdot \cos \phi' \quad (1)$$

$$\delta_{\text{film}} = \Delta S \cdot 2\pi / \lambda \quad (2)$$

The use of white light results in interference colors which are often more sensitive to small film thickness variations than the corresponding monochromatic intensity variations, and which admit an easy distinction between the first few orders of interference. The colors can be calibrated by comparison with monochromatic patterns in a continuously tapered film; thus, the characteristics of the photographic color material do not affect

the results. The observations on cylindrical electrodes are more difficult, but not basically different. A discussion of curved films has been given by Barakat.¹³

As had been noted by Blodgett and Langmuir^{14,15}, it is advantageous to use linearly polarized light to simplify the analysis of film interference. These authors also describe the improved contrast of an interference pattern when observed at a grazing angle of incidence. Similar observations are reported by Gaudin.¹⁶ A detailed analysis of interference in a transparent film on an absorbing substrate, which takes multiple reflections into account,¹⁷ shows that with light polarized parallel and normal to the plane of incidence (p and s polarization) "optimum angles of incidence" can be found for which the amplitudes of the interfering waves are equal, thus resulting in optimum interference contrast. The optimum angle of incidence is larger for p than for s polarization, it increases with increasing reflectivity of the metal substrate and decreases with increasing refractive index of the film. For many metal-film combinations 75° angle of incidence has been found to be a good intermediate value for observation with both s and p polarization.

For the quantitative interpretation of interference patterns in terms of film thickness, the phase change suffered by the light upon reflection at the two film boundaries has to be taken into account as pointed out e.g., by Mayer¹⁸ and discussed in a different context by Lindberg.¹⁹ The total phase difference δ between the interfering reflections is composed of a part δ_{film} due to the optical path in the film (taken negative as a relative delay in time) and the combined effect

$\delta_{\text{refl.}}$ of the reflections as expressed in Eq. (3). The latter quantity in turn represents the difference between the phase changes in dielectric and metallic reflections at the two film boundaries with respect to the incident wave (Eq. (4)).

$$\delta = \delta_{\text{film}} + \delta_{\text{refl.}} \quad (3)$$

$$\delta_{\text{refl}} = \delta_{\text{diel}} - \delta_{\text{metal}} \quad (4)$$

The phase changes in reflection affect the position of the origin of the film thickness scale deduced from the interference fringes, and become particularly significant for film thicknesses of a wavelength of light or less. If only the first two of the multiple reflections in the film are considered for a moment (R_0 and R_1 in Fig. 1), the phase relationships can be visualized in a vector diagram illustrated in Fig. 2. This representation shows phase and amplitude as angular and radial coordinates, respectively, and takes the time-independent phase of the incident wave E at the gas-film interface as a reference. For an aqueous 3.4 N KOH film ($n = 1.365$) on a nickel substrate and 75° angle of incidence ϕ on the film, for instance, (angle of incidence on the metal $\phi' = 45^\circ$) phase shifts δ_{metal} for the metallic reflection of 112° and 48° in the sense of a phase advance have been computed for s and p polarization, respectively, from the optical constants of the interface measured by ellipsometry.²⁰ These values are indicated by the positions of the vectors R_1 in Figs. 2a and b. The vectors R_0 show a 180° or 0° phase change, with s and p polarization, respectively, characteristic of the dielectric reflection at the gas-film interface under angles of incidence larger than Brewster's angle. Since a film of in-

creasing thickness increasingly delays reflection R_1 indicated by the double arrows in Figs. 2a and b, the sum of the two complex amplitudes R_0 and R_1 , a measure of the observed interference intensity, as a function of film thickness goes first through a minimum for s - polarization (Fig. 2c) but a maximum for p polarization (Fig. 2d). Thus, the interference patterns with the two polarizations are approximately complementary to each other. Because the characteristic interference fringes which can be used for a quantitative interpretation correspond to different film thicknesses in the two polarizations, the simultaneous use of both yields twice the number of measured contour lines.

Experimental

The electrolytic cells employed contained optically polished metal electrodes of rectangular (1.5 x 3 cm high) or cylindrical (2 x 13 cm high) geometry made of nickel or silver and inert counter electrodes of large surface area in separate cell compartments. Openings were provided to control the electrolyte level and maintain atmospheres of known composition in the cell volume not occupied by the liquid. The nitrogen or oxygen gas was kept water-saturated with solution of the bulk concentration. After careful mechanical degreasing, the electrodes were electrolytically cleaned by hydrogen evolution. It is important that every trace of grease be excluded from the cell, particularly in working with dilute solutions, where even deposits from the laboratory atmosphere have been found to spread from the outside of the cell through open ports onto the electrode surface. Most experiments were initiated by rapidly lowering the liquid level in the cell to 5 mm above the lower electrode edge and observing the subsequent drainage of the film as a function of time.

The optical arrangement used for this observation is given in Fig. 3 as a plan view diagram. Two collimated light beams A - F polarized parallel and normal to the plane of incidence are directed toward the film-covered surface G under an angle of incidence ϕ . The respective reflections are collected by two objectives L and placed by a set of first surface mirrors M side by side on the frame N of a 16 mm movie camera geared for single frame exposure. The image of a clock K was also placed on each frame by the objective I and the two mirrors H in order to record elapsed time. An automatic interval timer activated the camera shutter and turned the illumination off between exposures in order to avoid heating by light absorption.

Results

The evaluation of interference pictures from typical experiments along the vertical center line of the electrode results in film profiles given in Figs. 4a and b. After the initial drainage, a stationary film geometry is reached after a period in the order of ten hours. This period is shorter and the resulting stationary film is thicker for an oxygen-consuming electrode as compared to the same metal-solution system not electrochemically polarized. The stationary film geometry has been asserted not to change in selected experiments over periods of several weeks.

If viscous and gravitational forces only are considered for the thinning of the electrolyte film Eq. (5) can be derived²¹ for the dependence of film thickness d on vertical coordinate z (measured from the upper electrode edge down) and time t

$$d = (\mu/\rho g)^{1/2} z^{1/2} t^{-1/2} \quad (5)$$

where μ = viscosity, ρ = density, g = gravitational acceleration. Under these assumptions, a plot of film thickness vs inverse square root of time would result in a straight line through the origin for a given electrolyte composition and electrode position. Such an analysis of the previously shown film profiles (Fig. 4) 1 cm above the liquid level results in the curves of Fig. 5. It can be seen that the expected relationship holds down to about one micron film thickness. With no electrochemical polarization of the electrode (Fig. 5a), the rate of film thinning gradually deviates from that of a free-flowing liquid due to the effect of interfacial forces until a steady state value of 0.31 microns is reached after 20 hours. The film thinning with concurrent cathodic oxygen consumption under constant current (Fig. 5b) exhibits an abnormally rapid thinning rate before reaching a steady state value of 0.39 microns after 6 hrs. The rapid film thinning may be due to electro-osmotic effects, the establishment of a concentration profile and the non-uniformity of electro-chemical polarization. Two steady state film profiles measured on the same electrodes under different load are shown in Fig. 6a. The response of film thickness to changes in cathodic polarization occurs with a transition time in the order of 10 hrs. The same steady state profiles are attained from previously higher or lower polarization. Such changes can be expected to take place in fuel cell electrodes under variable load.

Stationary film profiles of KOH solution on nickel and silver, two electrode materials of practical interest, are compared in Fig. 6b. They reflect the different surface properties of the two metals.

The dependence of the steady state film thickness on the liquid composition has been investigated with different potassium hydroxide concentrations; the film thickness has been found to increase with increasing concentration.

For this reason, a 3.5N KOH film could be grown upward on a vertical nickel surface previously in equilibrium with distilled water, which forms a coverage just barely measurable by the interference method. Such a film growth, measured 1 cm above the liquid level, is illustrated in Fig. 7. It can be seen that the transition, again, takes in the order of 10 hours.

Discussion

The experiments conducted have established the geometry of stable electrolyte films on polished nickel and silver surfaces partially immersed in aqueous caustic solutions. The film geometry reflects a balance of interfacial forces and therefore depends on the properties of the liquid, those of the solid and the electrical potential applied between the two phases. A satisfactory theory of film behavior will have to take into consideration that stable configurations are reached both with and without reaction occurring in the film. Gradients of concentration and other properties in the film can be expected to affect its geometry but these do not seem to be the principal cause of film stability. The nature of the interfacial forces at play cannot be defined at present; however, it can be speculated on thermodynamic grounds for an equilibrium situation that with a typical heat of immersion of 100 ergs/cm^2 for metals in water, considerable energy is available for film formation, practically all of which is used for establishing the film-gas interface that typically requires 75 ergs/cm^2 .

While the electrolyte films studied are of a much simpler nature than those presumably existing inside certain porous gas diffusion electrodes, where the presence of capillary and pressure forces may lead to

different film geometries, the results obtained suggest further studies in this area. These include the practical significance of the unexpectedly long transition times to steady state, the effects of electrode surface pre-treatments and the complex interrelation of film geometry with the spatial distribution of current, potential, concentration and temperature in the film. Resulting changes in contact angle of the liquid meniscus inside capillary electrodes have been reported by Bonnemay et al.²² and oscillating phenomena suggested for this area²³ have recently been reported by Bockris et al.²⁴

The accuracy of the technique employed greatly depends on the optical properties of the substrate which determine the phase change in metallic reflection. These properties were computed from the complex refractive index of the solution-metal interface measured before and after each experiment. Various possibilities explored to check the phase relationships used in the evaluation of the interference fringes indicate a maximum error in film thickness of 0.1μ . The first such check is based on the dependence of the optical path ΔS in the film on the angle of refraction ϕ' expressed in Eq. (1). This dependence should extrapolate to zero for a given film viewed under different angles, and thus ascertain the origin of the film thickness scale. According to Snell's law, there is only a limited range of values which the angle of refraction can assume for the maximum variation in angle of incidence. Therefore, this test requires a long extrapolation and can detect only gross errors in phase (Fig. 8). It is, however, sensitive enough to reveal an error of a full interference order possible by a misinterpretation of fringes in the data evaluation. Another test can be based on the wavelength dependence of the film interference seen in Eq. (2) and requires observation of the same film

under a given angle of incidence with monochromatic light of different wavelengths. This presupposes a knowledge of the dispersion of the optical constants of metal and film. A third possibility consists in observing the sequence of interference colors as a film of a low solute content is rapidly evaporated to dryness by the introduction of a water-free gas phase. The variable refractive index of the film which represents another, although minor, source of error could possibly be determined by measuring Brewster's angle of incidence at which the interference pattern completely disappears in p polarization.¹⁷ Finally, ellipsometry offers the possibility of simultaneously determining refractive index and thickness of the film provided that the optical constants of the film-metal interface and the approximate value of the film thickness are known. This check will have to be performed at a later time.

Experiments are in progress with larger flat electrodes in order to approach the behavior of an infinitely extended surface suitable for the analysis of surface forces and the derivation of interfacial thermodynamic data. A detailed understanding of electrolyte films on polarized electrodes may permit one to derive the electrocapillarity of solid electrodes.

Acknowledgement

This work was performed under the auspices of the United States Atomic Energy Commission.

This paper has been presented in part at the Toronto Meeting, May 1964 and at the Washington Meeting, October 1964.

REFERENCES

1. W. R. Grove, *Phil. Mag.*, 21, 417 (1842).
2. F. G. Will, *This Journal*, 110, 145, 152 (1963).
3. A. Schmid, *Diss. Basel 1922*, Union Deutsche Verlagsgesellschaft, Stuttgart, 1923.
4. E. W. Justi, A. W. Winsel, Kalte Verbrennung, Fuel Cells, Steiner Verlag, Wiesbaden (1962), p. 89 ff.
5. R. P. Iczkowski, *This Journal*, 111, 1078 (1964).
6. D. N. Bennion, C. W. Tobias, Paper presented at the Washington Meeting, *Electrochem. Soc.*, Oct. 12, 1964.
7. H. J. R. Maget, R. Roethlein, *This Journal*, 112, 1034 (1965).
8. J. A. Rockett, Paper presented at the New York Meeting, *Electrochem. Soc.*, October 2, 1963.
9. E. A. Grens, R. M. Turner; T. Katan, *Advanced Energy Conversion*, 4, 109 (1964).
10. T. Katan, S. Szpak, E. A. Grens, *This Journal*, 112, 1166 (1965).
11. W. D. Bascom, R. L. Cottingham, C. R. Singleterry, in Contact Angle, Wettability and Adhesion, R. F. Gould, ed., p.355, *Am. Chem. Soc.*, Washington D. C. (1964).
12. B. V. Deryagin, N. N. Zakhavaeva, S. V. Andreev, A. A. Milovidov, A. M. Khomumov, in Research in Surface Forces, B. V. Deryagin, ed., p. 110, Consultants Bureau, New York, (1963).
13. N. Barakat, *J. Opt. Soc. Amer.*, 48, 92 (1958).
14. K. B. Blodgett, *J. Phys. Chem.*, 41, 975 (1937).
15. K. B. Blodgett, *I. Langmuir, Phys. Rev.*, 51, 964 (1937).
16. A. M. Gaudin, *J. Phys. Chem.*, 41, 811 (1937).
17. R. H. Muller, *J. Opt. Soc. Amer.*, 54, 419 (1964), also Lawrence Radiation Laboratory Report UCRL-10963, July 1963.

18. H. Mayer, Physik duenner Schichten, p. 54, Wiss. Verlagsges, Stuttgart (1950).
19. P. J. Lindberg, Optica Acta 4, 59 (1957).
20. W. Koenig in Handbuch der Physik, H. Geiger, K. Scheel, ed., Vol. 20 p. 242, 243, Verlag Julius Springer, Berlin (1928), also R. H. Muller, J. R. Mowat, Lawrence Radiation Laboratory Report UCRL 11813, to be issued..
21. R.B.Bird, W.E.Stewart, E.N.Lightfoot, Transport Phenomena, J. Wiley and Sons, Inc., (1960); D. N. Bennion, Thesis, Dept. of Chem. Engr., University of California, June 1964.
22. M. Bonnemay, G. Bronoel, E. Levant, Electrochim. Acta 9, 727 (1964).
23. R. H. Muller, Paper presented at the Washington Meeting, Electrochem. Soc., October 12, 1964, Extended Abstract No. 4.
24. J. O'M. Brockris, L. Nanis, B. D. Cahan, J. Electroanal. Chem. 9, 474 (1965).

- 4 -

FIGURE CAPTIONS

Fig. 1 Multiple beam interference from a transparent film on a metal substrate E = incident wave, R = reflected waves, ϕ = angle of incidence on the film, ϕ' = angle of refraction in the film.

Fig. 2 Effect of phase changes in dielectric and metallic reflection on double beam film interference. (a), (b) vector representation of phase relationships between interfering waves R_0 and R_1 shown in Fig. 1, (c), (d) predicted interference intensity distribution in a wedge shaped film.

Fig. 3 Optical arrangement for slow motion movies photography of film formation. A = lamp, B = condenser, C = iris diaphragm, D = neutral density and color correction filters, E = collimator lens, F = polaroid filters with transmitted electric vector in and normal to the plane of the drawing, G = film covered surface, H = mirrors, I = objective, K = face of clock, L = objectives, M = mirrors, N = photographic film.

Fig. 4 Formation of electrolyte films on flat nickel plates after partial withdrawal from 3.4N KOH solution, selected film profiles, h = vertical dimension of electrode, d = film thickness, LL = position of liquid level (a) cathodically polarized electrode ($65\mu\text{A}/\text{cm}$), oxygen atmosphere, (b) unpolarized electrode, nitrogen atmosphere.

Fig. 5 Deviations from purely gravitation drainage of 3.4N KOH film on polished nickel surface at small film thickness observed 1 cm above the liquid level. (a) unpolarized electrode, nitrogen atmosphere (b) cathodically polarized electrode ($65\mu\text{A}/\text{cm}$), oxygen atmosphere.

Fig. 6 (a) Stationary film profiles on flat (o) and cylindrical (Δ) nickel electrodes at different current densities. 3.5N KOH, O_2 .
(b) Stationary film profiles on different metals. 3.5N KOH, O_2 , $50\mu A/cm$.

Fig. 7 Film growth of 3.5N KOH on a vertical, unpolarized nickel surface previously covered with a stationary distilled water film, observed 1 cm above the liquid level.

Fig. 8 Interference in the same film under different angles of incidence. Extrapolation of optical path length at different film levels h to check phase changes used in evaluation.

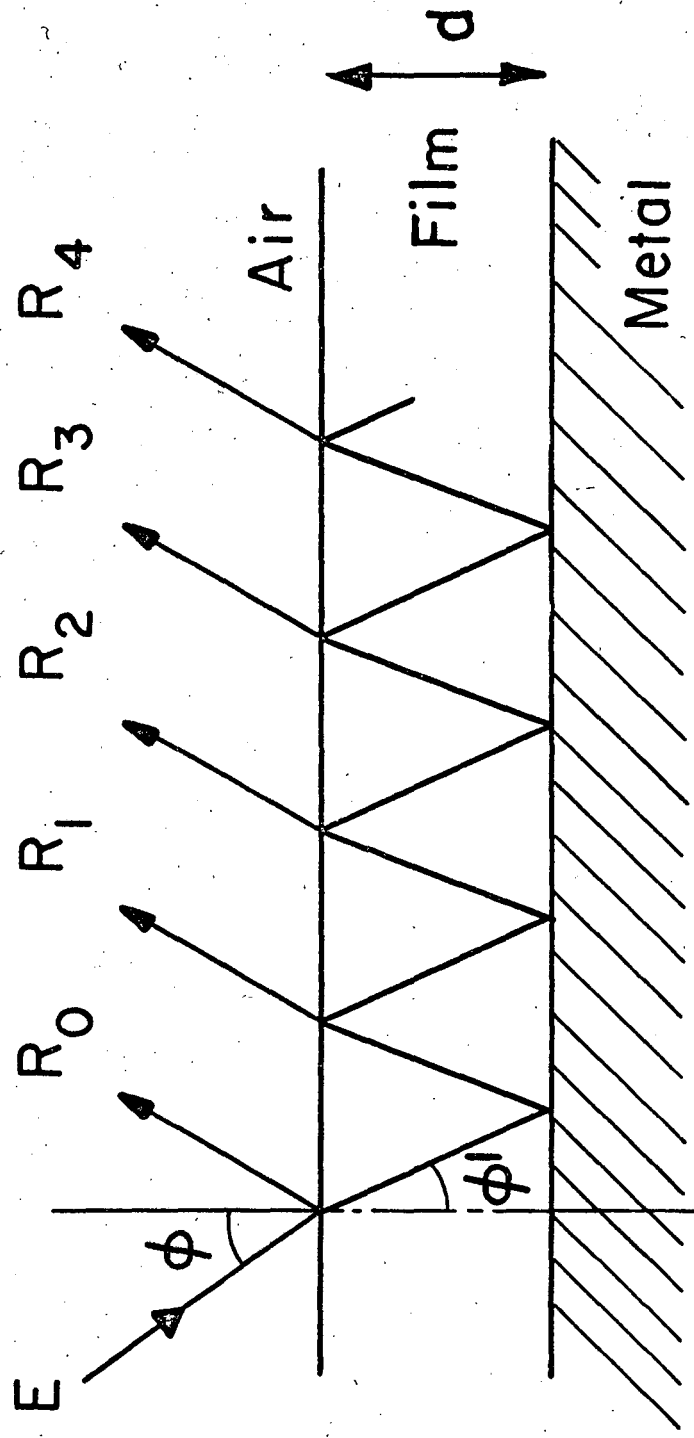
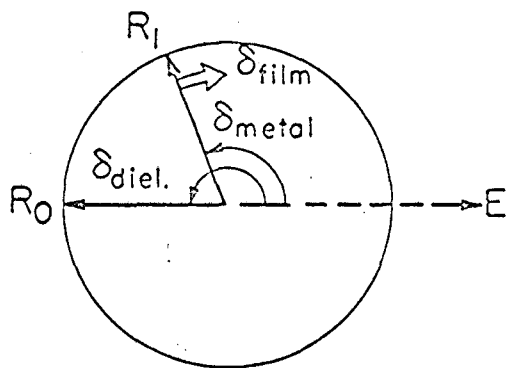


Fig. 1

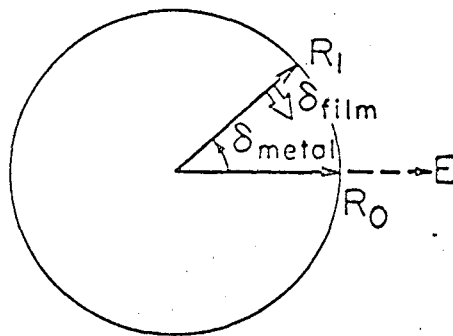
MU-31633-A

s-polarization (\perp)

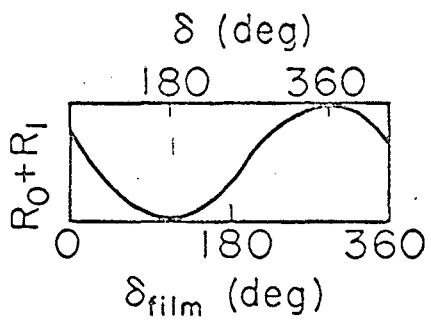
p-polarization (\parallel)



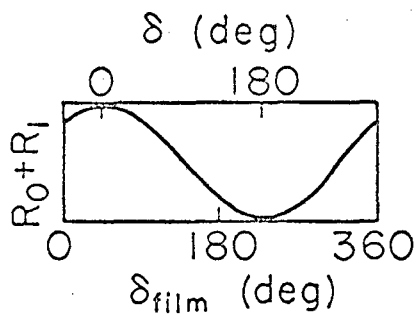
(a)



(b)



(c)



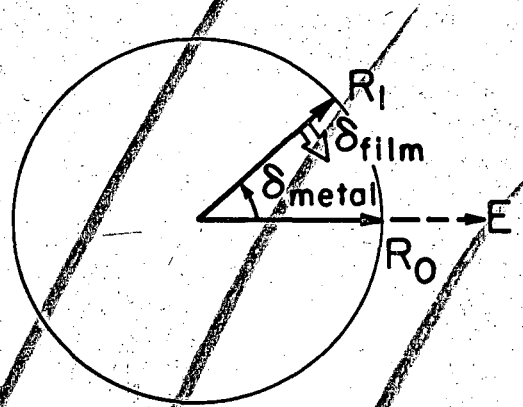
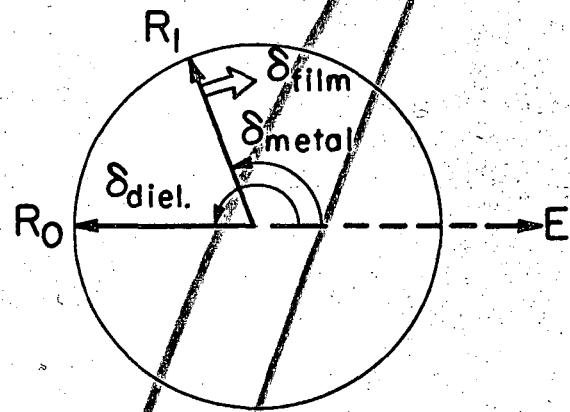
(d)

MUB-9179

Fig. 2

s-polarization (I)

p-polarization (II)



(a)

(b)

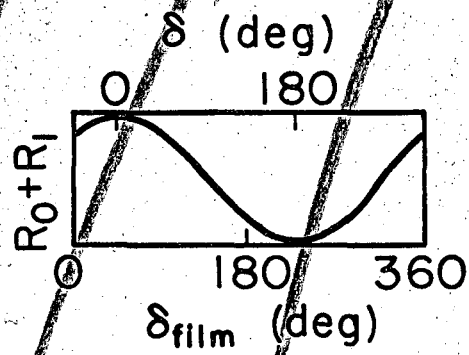
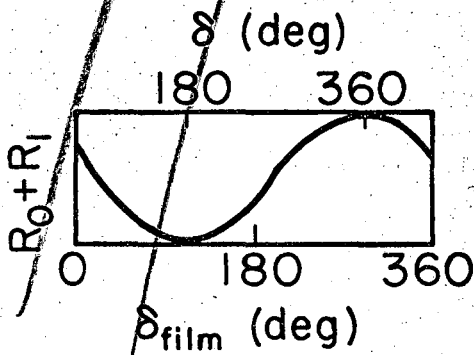


Fig. 2

MUB-9179

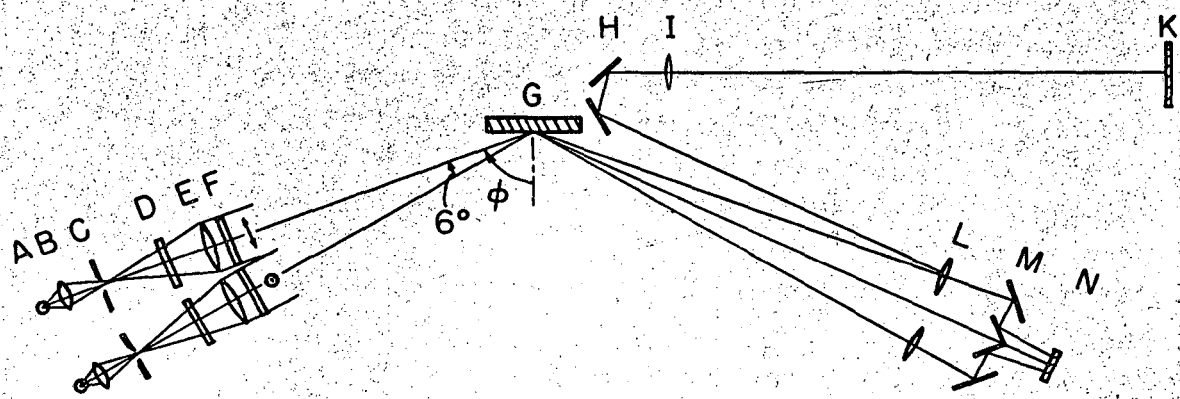


Fig. 3

MUB-9180

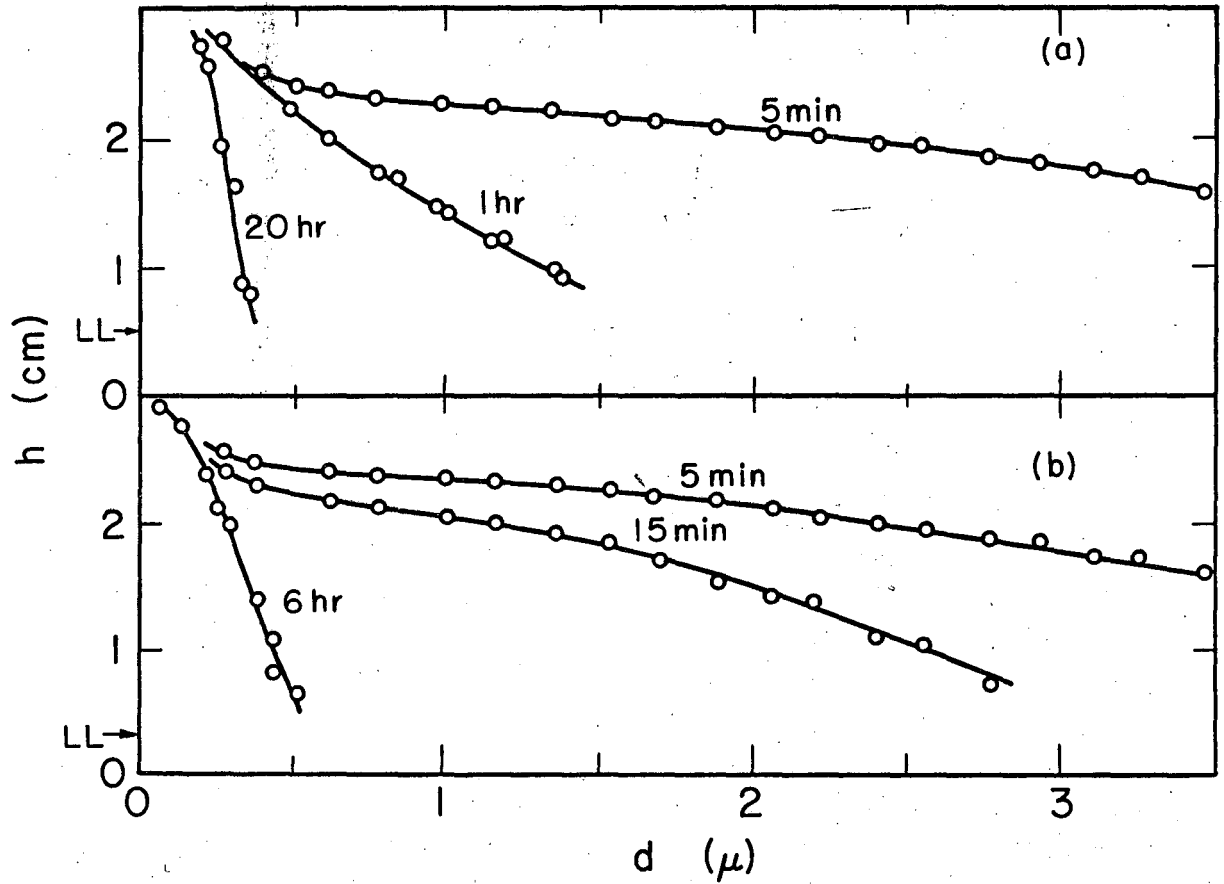


Fig. 4

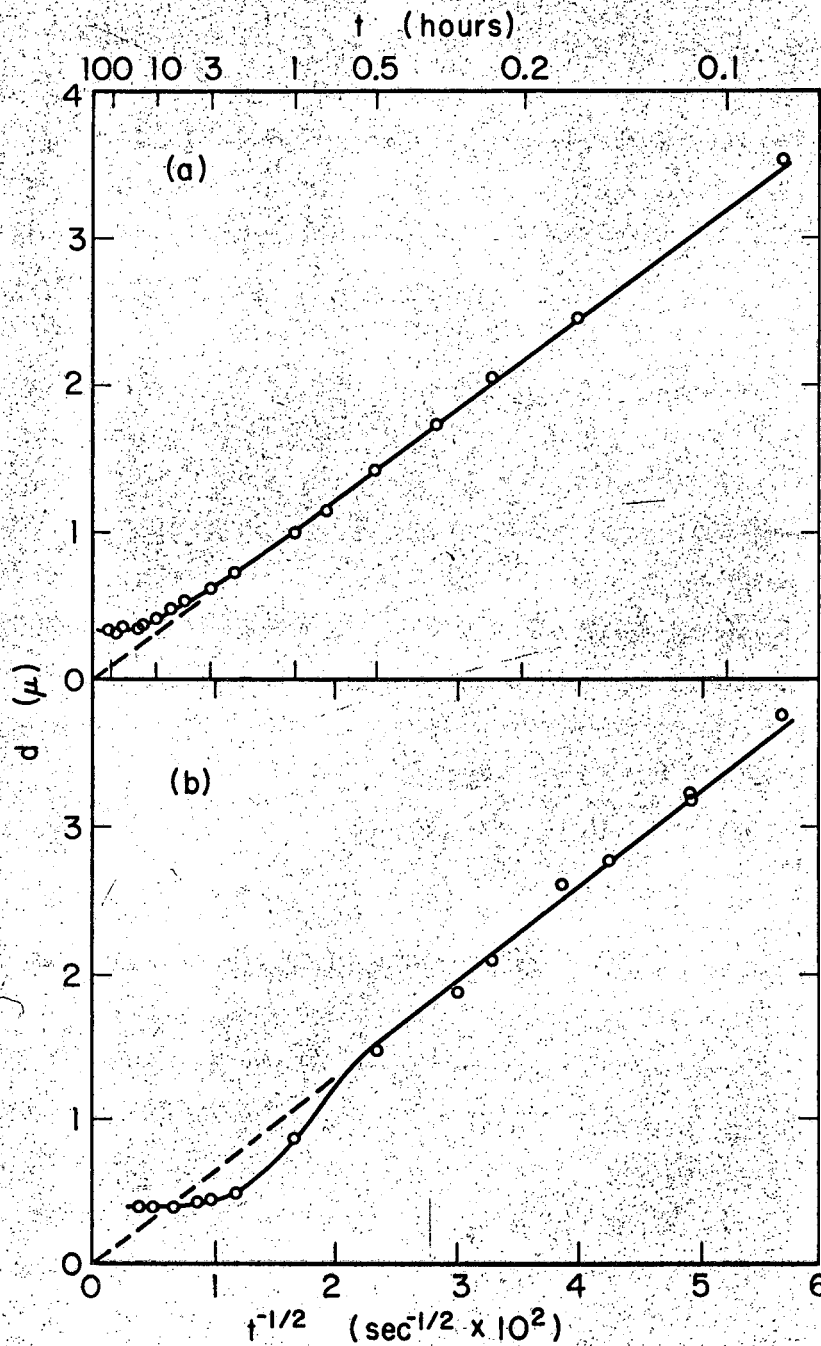


Fig. 5

MUB-9185

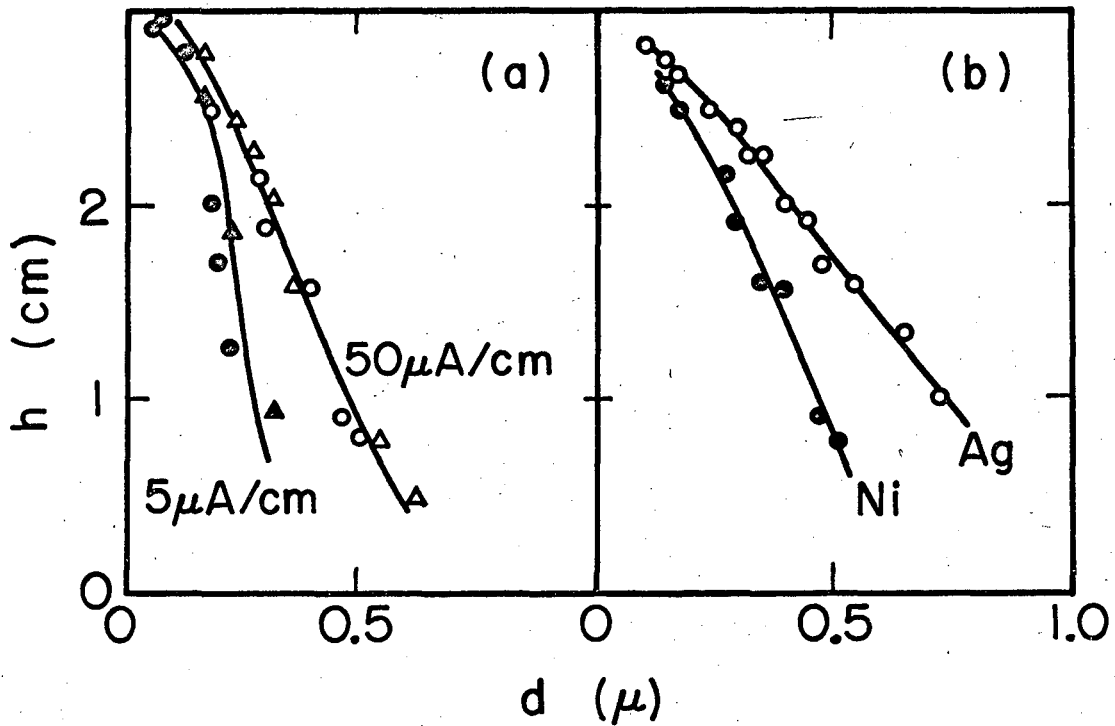


Fig. 6

MUB-9182

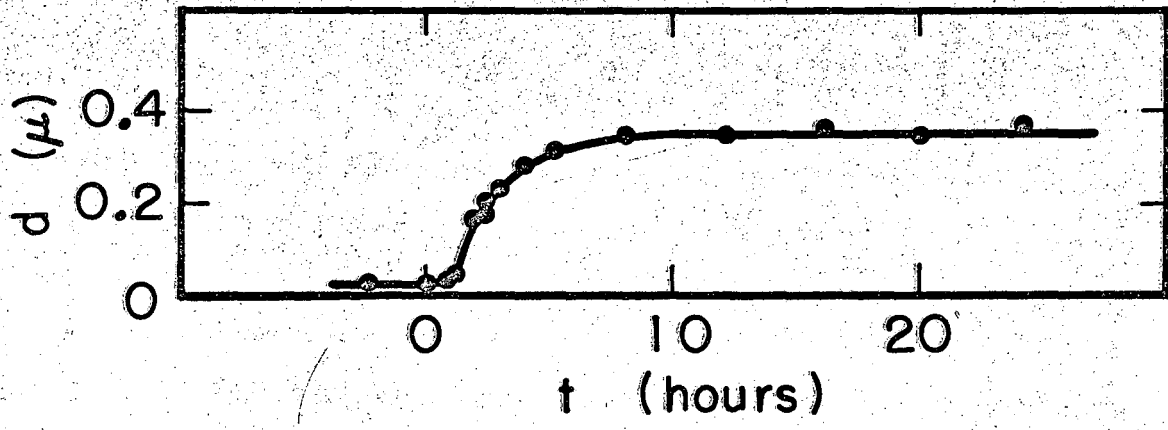


Fig. 7

MUB-9183

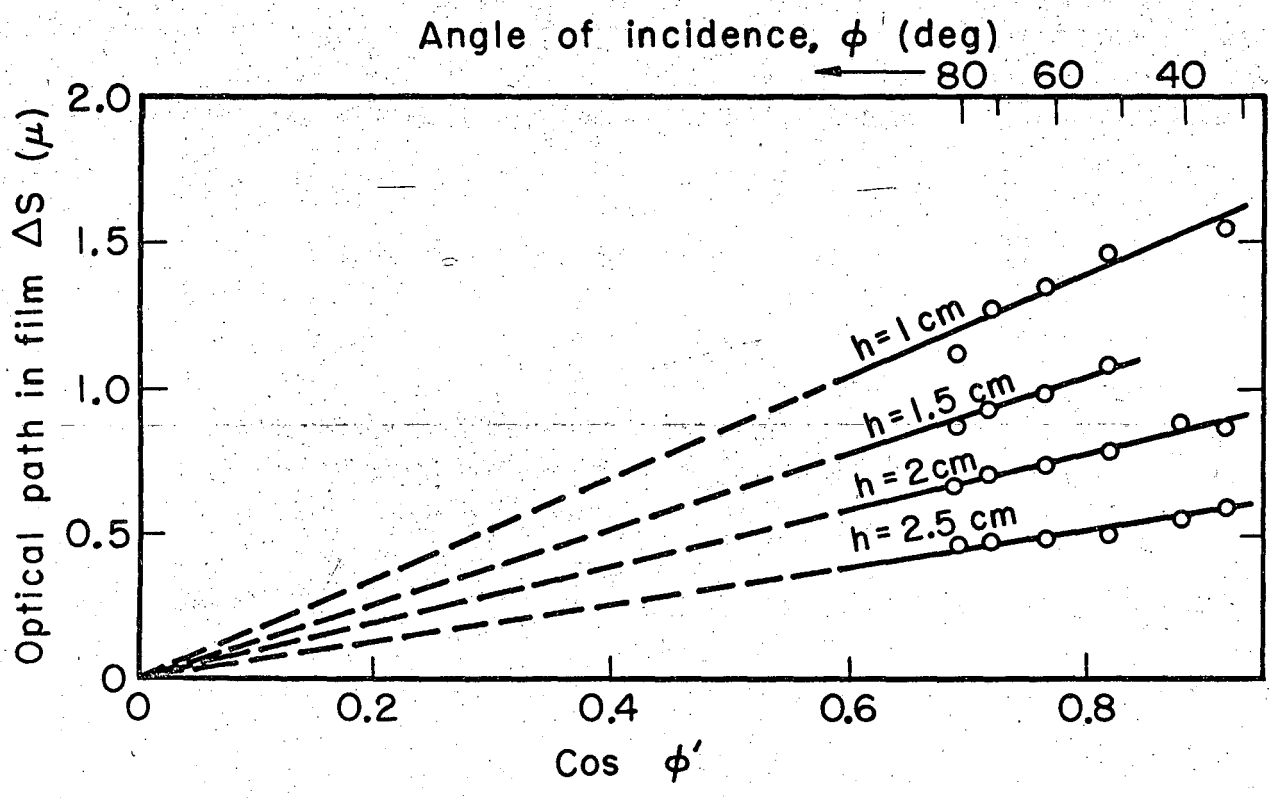


Fig. 8

MUB-9184

